Ecdysone Signaling at Metamorphosis Triggers Apoptosis of Drosophila Abdominal Muscles

Published in final edited form as:
Dev Biol. 2013 November 15; 383(2): 275–284. doi:10.1016/j.ydbio.2013.08.029.

Ecdysone signaling at metamorphosis triggers apoptosis of *Drosophila* abdominal muscles

Jonathan Zirin[1,*], **Daojun Cheng**[1,3], **Nagaraju Dhanyasi**[5,6], **Julio Cho**[1], **Jean-Maurice Dura**[4], **Krishnaswamy VijayRaghavan**[5], and **Norbert Perrimon**[1,2,*]

[1]Department of Genetics, Harvard Medical School

[2]Howard Hughes Medical Institute, 77 Avenue Louis Pasteur, Boston, Massachusetts 02115, USA

[3]State Key Laboratory of Silkworm Genome Biology, Southwest University, Chongqing, China

[4]Institute of Human Genetics, UPR 1142, CNRS. 141, rue de la Cardonille, 34396 Montpellier, France

[5]National Centre for Biological Sciences (NCBS)-TIFR, Bangalore, India

[6]Weizmann Institute of Science, Rehovot, Israel

Abstract

One of the most dramatic examples of programmed cell death occurs during *Drosophila* metamorphosis, when most of the larval tissues are destroyed in a process termed histolysis. Much of our understanding of this process comes from analyses of salivary gland and midgut cell death. In contrast, relatively little is known about the degradation of the larval musculature. Here, we analyze the programmed destruction of the abdominal dorsal exterior oblique muscle (DEOM) which occurs during the first 24 hrs of metamorphosis. We find that ecdysone signaling through Ecdysone receptor isoform B1 is required cell autonomously for the muscle death. Furthermore, we show that the orphan nuclear receptor FTZ-F1, opposed by another nuclear receptor, HR39, plays a critical role in the timing of DEOM histolysis. Finally, we show that unlike the histolysis of salivary gland and midgut, abdominal muscle death occurs by apoptosis, and does not require autophagy. Thus, there is no set rule as to the role of autophagy and apoptosis during *Drosophila* histolysis.

Introduction

Programmed cell death (PCD) describes the process by which a cell, through a regulated sequence of events, kills itself. This process is deployed in both plants and animals as a

*To whom correspondence should be addressed. jzirin@genetics.med.harvard.edu and perrimon@receptor.med.harvard.edu, Phone: 617-432-7672, Fax: 617-432-7688.

response to cell stress and as a means to eliminate extraneous cells during development (Conradt, 2009; Lockshin and Zakeri, 2007). PCD can refer to apoptosis, autophagy or programmed necrosis. Apoptosis, referred to as type I PCD, is characterized by caspase activation, cell shrinkage, membrane blebbing, nuclear condensation and DNA fragmentation, and finally loss of adhesion to extracellular matrix and phagocytic engulfment (Kerr et al., 1972). Autophagy, referred to as type II PCD, involves bulk degradation of organelles and long-lived proteins. Upon autophagy induction, a double membrane vesicle envelops the cytoplasm, then fuses with the lysosome, where its inner membrane and contents are degraded by hydrolases (Yang and Klionsky, 2009). Autophagy is not strictly a cell death pathway, as it facilitates the recycling of essential nutrients and energy during periods of starvation, and protects the cell from injuries caused by stress and infection. Finally, programmed necrosis, also known as type III PCD is a non-lysosomal type of cell death that has characteristics of necrosis, but is rarely observed (Clarke, 1990).

One of the most dramatic examples of PCD occurs during *Drosophila* metamorphosis. After hatching, the *Drosophila* larva spends the next 3 to 4 days feeding, growing and developing the imaginal tissues and other primodia which will ultimately form much of the adult body. During metamorphosis, most of the larval tissues are destroyed through PCD in a process termed histolysis (Baehrecke, 1996). The transitions between developmental stages in *Drosophila* are controlled by pulses of the steroid hormone 20-hydroxyecdysone (ecdysone) (Riddiford et al., 2000; Thummel, 2001). A high titer pulse of the hormone triggers the end of the larval stage and the transition to the puparium phase, and a subsequent pulse 12 hrs later triggers head eversion marking the beginning of the pupal phase (Thummel, 1996). Pupation lasts approximately 3.5 days, after which the adult fly emerges from the pupal case.

Our understanding of the signaling pathway leading to histolysis comes primarily from analyses of the salivary glands, which are destroyed in response to the ecdysone peak at the prepupal/pupal transition, respectively (Lee and Baehrecke, 2001; Lee et al., 2003; Lee et al., 2002b). Ecdysone binds to a heterodimeric receptor complex consisting of Ecdysone Receptor (EcR) and Ultraspiracle (USP) (Koelle et al., 1991; Thomas et al., 1993; Yao et al., 1992). This complex enters the nucleus and activates the transcription of the so-called early genes, including *Broad-Complex (BR-C)*, *E74A*, *E75*, and *E93* (Baehrecke and Thummel, 1995; Burtis et al., 1990; DiBello et al., 1991; Segraves and Hogness, 1990). The early genes, in turn activate transcription of a larger set of late genes/secondary response genes, which are thought to dictate the specific developmental output of the ecdysone signaling cascade (Thummel, 1995, 1996).

Another important player in the timing of salivary gland cell death is the orphan nuclear hormone receptor gene *ftz-f1 (βftz-f1)*, which is transcribed midway through prepupal development, when the ecdysone titer is relatively low (Lavorgna et al., 1993). In salivary glands, FTZ-F1 functions together with EcR to activate transcription of the early genes and subsequent cell death pathway in response to the ecdysone pulse at the prepupal/pupal transition (Broadus et al., 1999; Woodard et al., 1994). In addition to its role in salivary gland death, FTZ-F1 was recently shown to play a critical role during the ecdysone-dependent remodeling of fat body cells (Bond et al., 2011) mushroom body neurons, and

motor neuronsduring metamorphosis (Boulanger et al., 2011; Boulanger et al., 2012; Redt-Clouet et al., 2012; Sullivan and Thummel, 2003).

Much of the evidence for autophagic cell death comes from studies of salivary gland cell death during metamorphosis, which requires autophagy, although it remains unclear precisely how autophagy promotes death (Baehrecke, 2005; Berry and Baehrecke, 2007; Das et al., 2012). Additional evidence comes from studies of the midgut, which is destroyed in response to the ecdysone peak at the end of larval development (Lee et al., 2002a). Like salivary gland death, midgut histolysis also requires a functioning autophagy pathway (Denton et al., 2010; Denton et al., 2009). Less well studied than either salivary gland or midgut histolysis is the destruction of the larval muscles, which occurs first in the thoracic segments at the onset of puparium formation, then about 8–10 hrs later in the abdominal muscles (Bodenstein; Robertson, 1936).

Like the salivary gland and midgut, *Drosophila* produces distinct larval and adult sets of muscles. In the first 24 hrs after puparium formation (APF) most of the larval muscles have been completely degraded (Bate et al., 1991; Currie and Bate, 1991). A small set of muscles persist throughout metamorphosis, serving as templates for the morphogenesis of adult muscles, then die in the first two days after the adult fly ecloses (Dutta et al., 2002; Fernandes et al., 1991; Kimura and Truman, 1990; Roy and VijayRaghavan, 1998). Among these muscles are the dorsal internal oblique muscles (DIOMs), which lie just underneath the dorsal external oblique muscles (DEOMs) in each hemisegment of the abdomen (Currie and Bate, 1991; Wasser et al., 2007). These latter muscles are one of the few cases where the process of cell death has been examined in any detail during the first day of metamorphosis, when the vast majority of all larval muscles are destroyed (Wasser et al., 2007). Here, we extend these studies, answering major questions about the process of muscle histolysis, including the role of the ecdysone pathway and the roles that apoptosis and autophagy play in carrying out PCD. We use the DEOMs as a model to examine these issues in more detail, and show that although both autophagy and apoptosis occurs during DEOM histolysis, only the latter is required for muscle degradation. We show that destruction of these muscles is dependent on ecdysone signaling through the EcR-B1 isoform. Further, we show that FTZ-F1, opposed by another nuclear receptor, HR39, plays a critical role in the timing of DEOM histolysis.

Materials and methods

Fly Stocks

Fly stocks used were: *yw; Dmef2-Gal4* (Ranganayakulu et al., 1996); *Dmef2-Gal4* was recombined with *UAS-GFP-Atg8a* (Juhasz et al., 2008); $Hr39^{03508}$ *(Hr39-lacZ)* is a lethal lacZ enhancer trap insertion (Allen and Spradling, 2008); $Hr39^{neo8}$ (Allen and Spradling, 2008); *UAS-Hr39* (Boulanger et al., 2011); *UAS-ftz-f1* (Boulanger et al., 2011); Mhc^{weeP26} (Clyne et al., 2003); *ftz-f1* protein trap *(YB0007)*, from Flytrap (flytrap.med.yale.edu) (Buszczak et al., 2007). The following RNAi lines were obtained from the DRSC/TriP DRSC/TRiP at Harvard Medical School (http://www.flyrnai.org/TRiP-HOME.html): *white* (HMS0004); *Atg1* (JF02273); *Atg5* (HMS01244); *Atg18* (JF02898), and *ftz-f1* (JF02738 and HMS00019). Additional fly lines were obtained from the Bloomington stock center: *UAS-*

p35 (BL5073); *UAS-EcR-B1*^{DN} (BL6872); *UAS-EcR-B1 RNAi* (BL9329); *UAS-EcR RNAi*^{104} (targets all isoforms of EcR) (BL9327). Unless otherwise noted, flies were reared at 25°C.

Immunostaining and Antibodies

For whole-mount immunostaining of fly tissues, 3$_{rd}$ instar larval, prepupal, or pupal body wall muscles were dissected according to (Budnik et al., 2006) and fixed for 15 min in PBS with 4% formaldehyde. After washing in PBT (1× PBS + 0.1% Triton X-100), samples were incubated overnight with the following antibodies (in PBT): rabbit anti-cleaved caspase 3, 1:300 (Cell Signaling Technology); mouse anti-EcR-A (15G1a), 1:50 (Developmental Studies Hybridoma Bank, DSHB); mouse anti-EcR-B1 (AD4.4), 1:50 (DSHB); mouse anti-EcR-Common (DDA2.7), 1:50 (DSHB); rabbit anti-beta-galactosidase (anti β-Gal), 1:2000 (Cappel).. After incubation with primary antibodies, the samples were washed in PBT and incubated with Alexa-conjugated secondary antibodies (Molecular Probes, 1:1000) and Alexa 488, 594, or 633-conjugated phalloidin (1:1000) to visualize F-actin (Molecular Probes, 1:1000). Nuclei were visualized by DAPI staining (1 μg/ml). Samples were washed in PBT and mounted in 1:1 glycerol/PBS and images were acquired with a Leica SP2 laser scanning confocal microscope. For pupal staging, white prepupae were individually selected at 0hrs APF and age was determined relative to this point. All animals were maintained at 25°C.

Feeding Protocol, and Chloroquine Treatment

Unless otherwise noted, all fly crosses and larvae were maintained in vials containing ‘standard’ food composed of 16.5 g/L yeast, 9.5 g/L soy fluor, 71 g/L cornmeal, 5.5 g/L agar, 5.5 g/L malt, 7.5% corn syrup, 0.4% propionic acid, and 1.3% Tegosept. For starvation induced autophagy experiments 3$_{rd}$ instar larvae were individually selected and no more than 20 per experiment were transferred to ‘low nutrient food’ composed of 0.3× standard food. Likewise, for the rich food diet, no more than 20 larvae were transferred to ‘high nutrient food’ composed of standard food supplemented with 100g/L sucrose and 50g/L yeast. For each genotype, at least 4 larvae from at least two independent vials were analyzed. For drug treatments, chloroquine diphosphate salt (Sigma) was added to the food at 2.5 mg/ml.

TUNEL

TUNEL labelling was performed according to the manufacturer protocol (In Situ Cell Death Detection Kit, Roche). Briefly, prepupae were dissected in PBS, then fixed in 4% formaldehyde in PBS for 15 min. After being washed and permeabilized in PBT, the muscles were incubated for 45 minutes at 37°C in the TUNEL reaction. Samples were then rinsed 3× in PBT and 3× in PBS, mounted, and analysed by confocal microscope.

Transmission Electron Microscopy

White pre-pupae were marked and aged to the required developmental stage. Pupal muscles were dissected in Schneider’s insect medium and fixed using paraformaldehyde and glutaraldehyde (2.5% each) in 0.1M sodium cacodylate buffer (pH 7.4), followed by three washes in buffer alone. The samples were secondarily stained with 1%OsO_4 for 2hrs,

washed and incubated with 2% uranyl acetate in 50% alcohol. The samples were then taken through an alcohol dehydration series (50, 75, 94 and 100%), infiltrated using propylene oxide and resin, and embedded and polymerized using Epon 812 (EMS) for 48hrs. Ultra-thin sectioning (70–90nm) was performed using a Leica Ultra microtome UCT. Sections were stained with 1% aqueous uranyl acetate and lead citrate solutions, mounted on grids and imaged using a Tecnai T12 Spirit transmission electron microscope (FEI) equipped with an Eagle CCD camera (FEI). TIA software was used for image acquisition.

Results

Time course of abdominal muscle degeneration

To fluorescently mark the muscles and observe their morphology starting at pupariation, we used a transgenic fly line (weeP26) expressing a GFP-tagged Myosin heavy chain protein (Fig. 1, Fig. S1). Up to 4–6hrs APF, neither the DIOMs nor the DEOMs show any signs of deterioration (Fig. 1A, 1B). At 8hrs APF, however, we observed the first signs of degradation in the DEOMs (Fig. 1C), which, unlike the DIOMs, begin to round up with disorganized sarcomere structure (marked by GFP-Mhc). By 12hrs APF, following head eversion and the transition from prepupa to pupa, the DEOMs are almost completely degraded, with most of the tissue fragmented and dispersed (Fig. 1D). At this stage DIOM morphology and GFP-Mhc pattern remain largely intact, although the muscles are thinner and more compact compared to earlier timepoints.

To obtain a more detailed view of the changes in muscle structure during histolysis of the DEOMs compared to the DIOMs, we analyzed the muscles by transmission electron microscopy (EM). At 0hrs APF, both the DIOMs and DEOMs have well-ordered sarcomere structures, with clearly defined Z-disc, A-band and I-band (Fig. 1E, 1I). At 4–6hrs APF both types of muscles retain their sarcomere structures, although sarcoplasmic reticulum and vesicles appear more frequently in the slightly expanded intermyofibrillar spaces of the DEOMs (Fig. 1F, 1J). At 8hrs APF the myofibrils of the DEOMs are still present, but are no longer aligned into well-ordered sarcomeres (Fig. 1K). The DIOMs at the same stage maintain an orderly sarcomere structure (Fig. 1G). Finally, by 12hrs APF, the DEOM myofibrils are mostly degraded (Fig. 1L), while the DIOM myofibrils are undegraded but abnormally aligned (Fig. 1H). Combined with the data obtained by confocal microscopy, these EM pictures clearly show that the major part of the DEOM histolysis occurs between 8 and 12hrs APF, during which time the muscles disintegrate and the myofibrils are degraded.

Abdominal muscle histolysis is apoptotic, not autophagic

Previous studies of histolysis during *Drosophila* metamorphosis have shown that both apoptosis and autophagy play different roles during PCD, depending on the particular tissue. We therefore examined the roles of these two processes during DEOM histolysis (Fig. 2, Fig. S5). We first stained the abdominal muscles with α-human cleaved caspase-3, which recognizes multiple apoptotic proteins in *Drosophila*, and serves as a marker for the activity of the initiator caspase Dronc (Fan and Bergmann, 2010). In control muscles expressing a *white* dsRNA using the muscle specific *Dmef2-Gal4* driver line, neither the DIOMs nor the DEOMs show any caspase-3 staining at 0hrs APF (Fig. 2A). At 8hrs APF however (Fig.

2B), consistent with previous reports (Wasser et al., 2007), caspase-3 stains the DEOMs as they begin to histolyze, and the staining persists during muscle fragmentation (Fig. 2C) through their complete histolysis (Fig. 2D). During this period the DIOMs never stain positive for caspase-3 (Fig. 2A–D). In addition, EM analysis of DEOMs at 8hrs APF revealed nuclei with condensed chromatin, one of the hallmarks of apoptosis (Fig. 2M), although it is notable that the extent of condensation is not as severe as in other apoptotic cell types. This may be due to the unusual size of these nuclei, which have been growing via endoreplication throughout the larval stage. DNA fragmentation, identified by TUNEL, was also observed in DEOM, but not DIOM, nuclei at this time point (Fig. 2O) further implicating the apoptotic pathway during DEOM histolysis. Finally, we tested whether blocking apoptosis would be sufficient to halt DEOM degradation. Strikingly, overexpression of the caspase inhibitor p35 under control of *Dmef2-Gal4* abolished caspase-3 staining and strongly inhibited DEOM histolysis and sarcomere degradation (Fig. 2E–H, P).

Studies in yeast have identified over 30 ATG (autophagy-related) genes, many of which are conserved in *Drosophila* and other higher organisms (Chang and Neufeld, 2011; Yang and Klionsky, 2011; Yorimitsu and Klionsky, 2005; Zirin and Perrimon, 2010). In all eukaryotes, autophagy requires a functioning autophagy-related gene 1 (Atg1) complex. We therefore knocked down *Atg1* specifically in muscles to determine whether, like apoptosis, autophagy is involved in the degradation of the DEOMs. In *Dmef2-Gal4/UAS-Atg1 RNAi* animals we observed no delay in either caspase staining or muscle degradation, which both began at 8hrs APF, and continued as in control *white* RNAi muscles (Fig. 2I–L). We obtained the same results with RNAi targeting other essential autophagy components Atg5 and Atg18 (data not shown). Additionally, each of these RNAi transgenes strongly inhibited autophagosome formation in larval muscles, indicating that these reagents are effective at blocking autophagy (Fig. S2). We also tested whether autophagosome formation was altered in the degrading muscles. Double and single membrane vesicles containing cytoplasm were observed in EM from DEOMs beginning at 6–8hrs APF, suggesting increased autophagic/lysosomal activity (Fig. 2N, Fig. S6). Finally, localization of a GFP-tagged version of the conserved ubiquitin-like protein Atg8 (Mizushima et al., 1998) was altered in the DEOMs relative to DIOMs, although we were unable to discern the formation of GFP labeled autophagosomes in the histolyzing muscle (Fig. S2). Taken together, these results indicate that while autophagy may be increased in DEOMs, it is not required for either caspase activation or the degradation of this tissue.

Ecdysone signaling is required for abdominal muscle histolysis

Ecdysone signaling has been studied extensively in tissues destined for degradation or remodeling during *Drosophila* metamorphosis (Bond et al., 2011; Cherbas et al., 2003; Jiang et al., 1997; Jiang et al., 2000; Lee and Baehrecke, 2001; Lee et al., 2003; Lee et al., 2002a; Lee et al., 2002b; Winbush and Weeks, 2011). However, the role of this pathway during abdominal muscle histolysis has not been tested. There are three different isoforms of the *EcR* gene, EcR-A, EcR-B1, and EcR-B2, each sharing the same DNA-binding and ligand-binding domains, but with a unique amino terminus (Talbot et al., 1993). We first analyzed EcR expression during abdominal muscle degeneration using antibodies specific to either

EcR-A or EcR-B1 isoforms. Both DEOMs and DIOMs express EcR-B1 throughout the period of muscle histolysis (Fig. 3A–D), while EcR-A was not expressed in either muscle type (Fig. S3). We did not have an antibody that specifically recognizes EcR-B2, however, an antibody that recognizes all EcR isoforms gave a staining pattern similar to α-EcR-B1 (Fig. S3), indicating that EcR-B2 is either absent from the muscles or has a pattern of expression similar to EcR-B1. Consistent with the expression data, knockdown of EcR-B1 using *Dmef2-Gal4* caused a delay of DEOM degradation and caspase activation (Fig. 3E–H, Fig. S5). Further, knockdown with an RNAi reagent targeting all EcR isoforms resulted in an even more substantial block of degradation (Fig. 3I–J, Fig. S5), as did overexpression of a dominant negative EcR-B1 transgene (Fig 3K–L, Fig. S5). Given these results, we can not rule out the possibility that EcR-B1 and EcR-B2 have some redundancy of function, which could account for the stronger phenotype in the dominant negative or all-isoform knockdown experiments.

FTZ-F1 is required for the proper timing of muscle histolysis

The stage specific expression of transcription factors is a critical determinant of the response of cells to the ecdysone signal during metamorphosis. In particular, the orphan nuclear receptor FTZ-F1 is subject to extensive regulation by the ecdysone signaling pathway during the prepupal stage, and is essential for the induction salivary gland histolysis (Thummel, 2001). We therefore examined whether FTZ-F1 similarly establishes the response of the abdominal muscle cells to the ecdysone signal. To follow the expression of FTZ-F1, we used the protein trap line YB0007, in which GFP-tagged *ftz-f1* is expressed under the control of its endogenous promoter and enhancer elements (Buszczak et al., 2007). At 0hrs APF, FTZ-F1-GFP is not expressed in either the DIOMs or DEOMs (Fig. 4A). At 5hrs APF we observed strong FTZ-F1-GFP expression in the DEOMs, but none in the DIOMs (Fig. 4B). The fusion protein is localized primarily to the nucleus, consistent with its role as a transcription factor. Expression of FTZ-F1-GFP is maintained in the dying DEOMs at 8hrs APF, when it also appears in DIOMs, persisting in these muscles through 16hrs APF (Fig. 4C–E). Thus, FTZ-F1 expression is differentially regulated in the dying and persistent muscles, and could therefore be an important determinant of their different responses to the ecdysone signal. To test this hypothesis, we knocked down *ftz-f1* specifically in muscles using *Dmef2-Gal4*, and examined the death of DEOMs. Strikingly, we consistently observed a delay in the activation of caspase and the death of DEOMs in the *ftz-f1* RNAi muscles (Fig. 4O–R, Fig. S5) compared to *white* RNAi control muscles (Fig. 4. K–N, Fig. S5). In many cases, the DEOMs persisted through 16hrs APF with no detectable caspase staining (Fig. 4R, Fig. S5). When we overexpressed FTZ-F1, the DEOMs degenerated prematurely, and the DIOMs had significant sarcomere disruption and reduced size (Fig. 4S–V, Fig. S5). However, FTZ-F1 overexpression was unable to induce early caspase activity in the DEOMs (Fig. 4S) or any caspase activity in the DIOMs (Fig. 4S–V), indicating that FTZ-F1 expression alone is not sufficient to trigger apoptosis of the abdominal muscles. It was recently shown that EcR-B1 expression depends on FTZ-F1 expression in the neurons of the mushroom body during metamorphosis (Boulanger et al., 2011). Given that we demonstrated that both *ftz-f1* and *EcR-B1* are essential for the proper histolysis of DEOMs, we examined the expression of EcR-B1 in *ftz-f1* RNAi muscles (Fig. S4). Unlike the

mushroom body system, however, we could not detect changes in EcR-B1 staining upon *ftz-f1* knockdown.

HR39 opposes FTZ-F1 function during muscle histolysis

Like FTZ-F1, the nuclear receptor gene HR39 is expressed during metamorphosis in response to ecdysone (Horner et al., 1995). Both of these factors have a high degree of sequence similarity, can bind to the same DNA sequence, and regulate some of the same genes (Ayer et al., 1993; Ohno et al., 1994). Interestingly, *Hr39* and *ftz-f1* are expressed at roughly reciprocal timepoints in the prepupae, and have opposing phenotypes during mushroom body and motor neuronal remodeling (Boulanger et al., 2011; Boulanger et al., 2012; Redt-Clouet et al., 2012; Sullivan and Thummel, 2003). We hypothesized that, since FTZ-F1 plays an important role in promoting abdominal muscle histolysis, HR39 might play the opposite role. We first examined the expression patter of *Hr39* using a *lacZ* reporter (Fig. 4F–J). At 0hrs APF, *Hr39-lacZ* is expressed strongly in the DIOMs, and much more weakly in the DEOMs (Fig. 4F). At 5hrs APF, when FTZ-F1 is present in the DEOMs, but absent in the DIOMs, *Hr39-lacZ* has the opposite pattern, with only weak expression in the DEOMs and high expression in the DIOMs (Fig. 4G). From 8–16hrs APF *Hr39-lacZ* expression continues in the persistent DIOMs (Fig. 4H–J). Next, we overexpressed HR39, and found that it was able to repress DEOM histolysis and caspase activity (Fig. 4W–Z), much like in *ftz-f1* knockdown muscles (Fig. 4. O–R). Conversely, *Hr39* mutant larvae prematurely activated caspase, hastening the degradation of the DEOMs (Fig. 5A–E, Fig. S5). By 5hrs APF (Fig. 5B), the DEOMs showed strong caspase activity, and the muscles were almost completely degraded by 8hrs APF (Fig. 5C). However, reduced *Hr39* had no apparent effect on the DIOMs (Fig. 5A–E). Finally, we examined the effect of muscle specific *ftz-f1* knockdown in the *Hr39* mutant animal to determine the epistatic relationship of the two genes. With respect to DEOM degradation, we found no difference between *ftz-f1* knockdown in the *Hr39* mutant trans-heterozygotes (Fig. 5K–O, Fig. S5) compared to *ftz-f1* knockdown in control *Hr39/+* heterozygotes (Fig. 5F–J, Fig. S5). That is, *ftz-f1* knockdown inhibited caspase activity and DEOM histolysis, irrespective of the *Hr39* background. Altogether, we conclude that *ftz-f1* is epistatic to *Hr39*, consistent with the view that FTZ-F1 expression is the ultimate determinant of DEOM death during metamorphosis.

Discussion

Ecdysone signaling is essential for histolysis of salivary gland and midgut, as well as for tissue remodeling during *Drosophila* metamorphosis (Bond et al., 2011; Cherbas et al., 2003; Jiang et al., 1997; Jiang et al., 2000; Lee and Baehrecke, 2001; Lee et al., 2003; Lee et al., 2002a; Lee et al., 2002b; Winbush and Weeks, 2011). However, the role of this pathway during abdominal muscle death had not previously been tested. There has been at least one report of ecdysone-independent PCD during metamorphosis (Hara et al., 2013) raising the possibility that muscle histolysis could be due to a different signaling pathway. In this study, we found that by knocking down all EcR isoforms specifically in the muscles, we could block muscle degradation, and that ectopic expression of a dominant negative EcR-B1 isoform had the same effect, indicating that the ecdysone pathway functions cell-autonomously in the muscle to promote cell death during metamorphosis.

There are three different isoforms of the *EcR* gene, EcR-A, EcR-B1, and EcR-B2, each sharing the same DNA-binding and ligand-binding domains, but with a unique amino terminus (Talbot et al., 1993). The different temporal and spatial expression patterns of EcR-A and EcR-B isoforms are thought to reflect their distinct functions during development (Davis et al., 2005; Truman et al., 1994). EcR-B1 is expressed primarily in larval cells that are destined for histolysis, while EcR-A is expressed primarily in imaginal tissues destined for differentiation into adult structures (Talbot et al., 1993). Thus the response of salivary glands and midgut to ecdysone during metamorphosis is dependent on EcR-B1 (Bender et al., 1997). Nonetheless, EcR-A mutants also have a defect in salivary gland histolysis, suggesting that the isoform might also contribute to this process (Davis et al., 2005). Furthermore, some neurons in the ventral nerve cord and brain that strongly express EcR-A undergo apoptosis in response to ecdysone soon after eclosion, suggesting that ecdysone induced PCD is not strictly a function of EcR-B1 signaling (Kato et al., 2009; Robinow et al., 1993).

We examined expression of both EcR-A and EcR-B1 isoforms and found that only EcR-B1 was detectable in the DIOMs and DEOMs during pupariation. Consistent with its expression pattern, knockdown of EcR-B1 specifically in the muscle inhibited DEOM histolysis. The inhibition achieved with the EcR-B1 isoform RNAi was not as strong as with RNAi targeting all isoforms, nor with overexpression of the dominant negative EcR-B1. This could be due to either differences in the efficiency of knockdown or to a role for EcR-B2 in DEOM degradation. Taken together our data strongly supports the view that, like in salivary glands and midgut, ecdysone signals through EcR-B1 to induce cell death in abdominal muscles. However, given that both DIOMs and DEOMs express EcR-B1 at the same time, the presence of the receptor is not sufficient to explain why only the latter muscles are degraded.

Another important player in the timing of salivary glands cell death is the orphan nuclear hormone receptor gene *ftz-f1*, which is transcribed midway through prepupal development, when the ecdysone titer is relatively low (Lavorgna et al., 1993). FTZ-F1 has been hypothesized as a competence factor, directing the subsequent genetic responses to the ecdysone pulse at the prepupal/pupal transition (Broadus et al., 1999; Woodard et al., 1994). Thus FTZ-F1 is required for the induction of salivary gland histolysis. In contrast, the midgut does not express *ftz-f1* prior to its earlier ecdysone induced cell death (Lee et al., 2002a), indicating that FTZ-F1 is not required for all histolysis during *Drosophila* metamorphosis. We found that despite the fact that the timing of muscle histolysis is similar to that of the midgut, the function of FTZ-F1 was more like in the salivary gland, as FTZ-F1 was observed in the DEOMs starting at ~5hrs APF, prior to caspase activation at 8hrs APF. Furthermore, *ftz-f1* was required for proper muscle histolysis, as knockdown cell-autonomously delayed caspase activation and death in the DEOMs.

These results raised the possibility that the presence of FTZ-F1 in the DEOMs, but not in the DIOMs, determined the different response of these muscles to ecdysone. However, overexpression of FTZ-F1 in the DIOMs, while causing severe muscle degeneration, was unable to induce caspase activity or cell death. Nor could the presence of HR39 in the DIOMs account for the different response of the muscles to ecdysone. Although we

observed a reciprocity of HR39 and FTZ-F1 expression in the DIOMs and DEOMs, Hr39 mutant DIOMs still persist through metamorphosis. We conclude that FTZ-F1 and HR39 expression determine the timing of the abdominal muscle response to ecdysone but that these factors do not change the nature of the response.

It was recently shown that EcR-B1 expression is regulated by FTZ-F1 and HR39 in mushroom body neurons and abdominal motor-neurons during metamorphosis (Boulanger et al., 2011; Boulanger et al., 2012). Our observation that EcR-B1 promotes muscle degeneration is consistent with the finding that EcR-B1 promotes post-synaptic dismantling in the motor-neuron, and supports the notion that muscle degeneration is instructive on motor neuron retraction. However, we show that even though both *ftz-f1* and *EcR-B1* are essential for the proper histolysis of DEOMs, there was no change in EcR-B1 staining upon *ftz-f1* knockdown as was observed in the mushroom body system. This suggests that changes observed in the muscle synapse due to *ftz-f1* knockdown are not the result of a downstream effect on EcR-B1 expression in the muscle cell. Thus, the regulatory relationship between FTZ-F1, HR39 and EcR-B1 in early pupal abdominal muscles is distinct from the relationship reported in neurons.

This suggests that there is an additional unknown factor whose expression dictates the fate of the DIOMs or DEOMs. This factor is unlikely to be either of the nuclear proteins EAST or Chromator (Chro), which were previously identified as having opposing effects on the destruction of the abdominal DEOMs during metamorphosis (Wasser et al., 2007). Breakdown of DEOMs was incomplete in *Chro* mutants, and promoted in *east* mutants, leading to the proposal that Chro activates and EAST inhibits tissue destruction and remodeling. However, neither *east* nor *chro* alleles cause histolysis of the DIOMs, nor do they alter caspase activation in either DEOMs or DIOMs. Rather these genes may affect the timing of muscle histolysis through a function downstream of PCD induction. We propose that there must be an additional factor present in the DIOMs which inhibits EcRB1 signaling from inducing PCD, or alternatively, a factor present in the DEOMs, which permits EcRB1 to activate a death program. The identification of this factor will be a focus of future studies.

The previously reported cleaved caspase-3 staining in the DEOMs is, to our knowledge, the only data addressing the nature of abdominal muscle PCD prior to our study. We aimed to address whether muscle histolysis is apoptotic, autophagic or some combination of both. During salivary gland histolysis, several autophagy related genes (ATGs) are upregulated (Gorski et al., 2003; Lee et al., 2003), and mutations or knockdown of these ATGs specifically in the salivary gland inhibit the destruction of the tissue (Berry and Baehrecke, 2007). Caspase activation also occurs in the histolyzing salivary glands, but overexpression of the caspase inhibitor p35 only partially blocks salivary gland degradation (Lee and Baehrecke, 2001). Simultaneous inhibition of both autophagy and apoptosis in the salivary gland produces the strongest inhibition of death, suggesting that both pathways contribute to histolysis of this tissue (Berry and Baehrecke, 2007). In contrast to salivary gland histolysis, midgut histolysis requires autophagy but not caspase activity. Mutations or knockdown of ATGs inhibit midgut death, but p35 expression has no effect (Denton et al., 2010; Denton et al., 2009). Based on these two model systems, it appears that there is no set rule as to the role of autophagy and apoptosis during *Drosophila* histolysis.

Our data serves to further highlight how distinctive PCD for each of the tissues undergoing histolysis. We found that DEOMs stain positive for cleaved caspase-3, consistent with previous reports. We also observed TUNEL positive staining and chromatin condensation in the DEOMs at 8hrs APF, both markers of apoptosis. Importantly, we were able to suppress DEOM degradation by overexpression of the pan-caspase inhibitor p35, indicating that unlike the midgut, muscle histolysis is apoptotic. To determine whether the muscle PCD was autophagic in nature, we examined the DEOMs by EM. Although we observed some autophagic vesicles in the dying muscles, they were not abundant, nor was GFP-Atg8 localization to autophagosomes examined by confocal microscopy. We knocked down several essential components of the autophagic machinery, and observed no effect on the timing or extent of DEOM histolysis. Although knockdown efficiency is always a concern with RNAi experiments, each of the transgenes was able to strongly inhibit autophagosome formation in larval muscles. We are therefore confident that autophagy is not required for DEOM PCD, putting the abdominal muscle in the unique category of non-autophagic histolysis. In future studies it will be interesting to compare muscles, salivary gland, and midgut to determine why each tissue has a distinctive type of PCD.

Supplementary Material

Refer to Web version on PubMed Central for supplementary material.

Acknowledgments

This work was supported by a RO1 grant (5R01AR057352) to NP; and an F32 NIH Postdoctoral Fellowship (5F32GM082174-02) to JZ. NP is an investigator of the HHMI. The work of JMD is supported by an ARC grant (SFI20121205950).

All of the transmission electron microscopy work was performed at the Electron Microscopy Unit, Department of Chemical Research Support of the Weizmann Institute of Science. We thank the members of this unit for instruction and guidance. We are also grateful to Prof. Ben-Zion Shilo and Dr. Eyal Schejter of the Weizmann Institute Department of Molecular Genetics for their advice and support.

References

Allen AK, Spradling AC. The Sf1-related nuclear hormone receptor Hr39 regulates Drosophila female reproductive tract development and function. Development. 2008; 135:311–321. [PubMed: 18077584]

Ayer S, Walker N, Mosammaparast M, Nelson JP, Shilo BZ, Benyajati C. Activation and repression of Drosophila alcohol dehydrogenase distal transcription by two steroid hormone receptor superfamily members binding to a common response element. Nucleic Acids Res. 1993; 21:1619–1627. [PubMed: 8479913]

Baehrecke EH. Ecdysone signaling cascade and regulation of Drosophila metamorphosis. Archives of insect biochemistry and physiology. 1996; 33:231–244. [PubMed: 8913033]

Baehrecke EH. Autophagy: dual roles in life and death? Nature reviews. Molecular cell biology. 2005; 6:505–510. [PubMed: 15928714]

Baehrecke EH, Thummel CS. The Drosophila E93 gene from the 93F early puff displays stage-and tissue-specific regulation by 20-hydroxyecdysone. Developmental biology. 1995; 171:85–97. [PubMed: 7556910]

Bate M, Rushton E, Currie DA. Cells with persistent twist expression are the embryonic precursors of adult muscles in Drosophila. Development. 1991; 113:79–89. [PubMed: 1765010]

Bender M, Imam FB, Talbot WS, Ganetzky B, Hogness DS. Drosophila ecdysone receptor mutations reveal functional differences among receptor isoforms. Cell. 1997; 91:777–788. [PubMed: 9413987]

Berry DL, Baehrecke EH. Growth arrest and autophagy are required for salivary gland cell degradation in Drosophila. Cell. 2007; 131:1137–1148. [PubMed: 18083103]

Bodenstein D. The postembryonic development of Drosophila.

Bond ND, Nelliot A, Bernardo MK, Ayerh MA, Gorski KA, Hoshizaki DK, Woodard CT. ssFTZ-F1 and Matrix metalloproteinase 2 are required for fat-body remodeling in Drosophila. Developmental biology. 2011; 360:286–296. [PubMed: 21978772]

Boulanger A, Clouet Redt C, Farge M, Flandre A, Guignard T, Fernando C, Juge F, Dura JM. ftz-f1 and Hr39 opposing roles on EcR expression during Drosophila mushroom body neuron remodeling. Nat Neurosci. 2011; 14:37–44. [PubMed: 21131955]

Boulanger A, Farge M, Ramanoudjame C, Wharton K, Dura JM. Drosophila motor neuron retraction during metamorphosis is mediated by inputs from TGF-beta/BMP signaling and orphan nuclear receptors. PLoS One. 2012; 7:e40255. [PubMed: 22792255]

Broadus J, McCabe JR, Endrizzi B, Thummel CS, Woodard CT. The Drosophila beta FTZ-F1 orphan nuclear receptor provides competence for stage-specific responses to the steroid hormone ecdysone. Molecular cell. 1999; 3:143–149. [PubMed: 10078197]

Budnik V, Gorczyca M, Prokop A. Selected methods for the anatomical study of Drosophila embryonic and larval neuromuscular junctions. International review of neurobiology. 2006; 75:323–365. [PubMed: 17137935]

Burtis KC, Thummel CS, Jones CW, Karim FD, Hogness DS. The Drosophila 74EF early puff contains E74, a complex ecdysone-inducible gene that encodes two ets-related proteins. Cell. 1990; 61:85–99. [PubMed: 2107982]

Buszczak M, Paterno S, Lighthouse D, Bachman J, Planck J, Owen S, Skora AD, Nystul TG, Ohlstein B, Allen A, Wilhelm JE, Murphy TD, Levis RW, Matunis E, Srivali N, Hoskins RA, Spradling AC. The carnegie protein trap library: a versatile tool for Drosophila developmental studies. Genetics. 2007; 175:1505–1531. [PubMed: 17194782]

Chang YY, Neufeld TP. Autophagy takes flight in Drosophila. FEBS Lett. 2011; 584:1342–1349. [PubMed: 20079355]

Cherbas L, Hu X, Zhimulev I, Belyaeva E, Cherbas P. EcR isoforms in Drosophila: testing tissue-specific requirements by targeted blockade and rescue. Development. 2003; 130:271–284. [PubMed: 12466195]

Clarke PG. Developmental cell death: morphological diversity and multiple mechanisms. Anatomy and embryology. 1990; 181:195–213. [PubMed: 2186664]

Clyne PJ, Brotman JS, Sweeney ST, Davis G. Green fluorescent protein tagging Drosophila proteins at their native genomic loci with small P elements. Genetics. 2003; 165:1433–1441. [PubMed: 14668392]

Conradt B. Genetic control of programmed cell death during animal development. Annual review of genetics. 2009; 43:493–523.

Currie DA, Bate M. The development of adult abdominal muscles in Drosophila: myoblasts express twist and are associated with nerves. Development. 1991; 113:91–102. [PubMed: 1765011]

Das G, Shravage BV, Baehrecke EH. Regulation and function of autophagy during cell survival and cell death. Cold Spring Harbor perspectives in biology. 2012; 4

Davis MB, Carney GE, Robertson AE, Bender M. Phenotypic analysis of EcR-A mutants suggests that EcR isoforms have unique functions during Drosophila development. Developmental biology. 2005; 282:385–396. [PubMed: 15950604]

Denton D, Shravage B, Simin R, Baehrecke EH, Kumar S. Larval midgut destruction in Drosophila: not dependent on caspases but suppressed by the loss of autophagy. Autophagy. 2010; 6:163–165. [PubMed: 20009534]

Denton D, Shravage B, Simin R, Mills K, Berry DL, Baehrecke EH, Kumar S. Autophagy, not apoptosis, is essential for midgut cell death in Drosophila. Current biology: CB. 2009; 19:1741–1746. [PubMed: 19818615]

DiBello PR, Withers DA, Bayer CA, Fristrom JW, Guild GM. The Drosophila Broad-Complex encodes a family of related proteins containing zinc fingers. Genetics. 1991; 129:385–397. [PubMed: 1743483]

Dutta D, Bloor JW, Ruiz-Gomez M, VijayRaghavan K, Kiehart DP. Real-time imaging of morphogenetic movements in Drosophila using Gal4-UAS-driven expression of GFP fused to the actin-binding domain of moesin. Genesis. 2002; 34:146–151. [PubMed: 12324971]

Fan Y, Bergmann A. The cleaved-Caspase-3 antibody is a marker of Caspase-9-like DRONC activity in Drosophila. Cell Death Differ. 2010; 17:534–539. [PubMed: 19960024]

Fernandes J, Bate M, Vijayraghavan K. Development of the indirect flight muscles of Drosophila. Development. 1991; 113:67–77. [PubMed: 1765009]

Gorski SM, Chittaranjan S, Pleasance ED, Freeman JD, Anderson CL, Varhol RJ, Coughlin SM, Zuyderduyn SD, Jones SJ, Marra MA. A SAGE approach to discovery of genes involved in autophagic cell death. Current biology: CB. 2003; 13:358–363. [PubMed: 12593804]

Hara Y, Hirai K, Togane Y, Akagawa H, Iwabuchi K, Tsujimura H. Ecdysone-dependent and ecdysone-independent programmed cell death in the developing optic lobe of Drosophila. Developmental biology. 2013; 374:127–141. [PubMed: 23149076]

Horner MA, Chen T, Thummel CS. Ecdysteroid regulation and DNA binding properties of Drosophila nuclear hormone receptor superfamily members. Developmental biology. 1995; 168:490–502. [PubMed: 7729584]

Jiang C, Baehrecke EH, Thummel CS. Steroid regulated programmed cell death during Drosophila metamorphosis. Development. 1997; 124:4673–4683. [PubMed: 9409683]

Jiang C, Lamblin AF, Steller H, Thummel CS. A steroid-triggered transcriptional hierarchy controls salivary gland cell death during Drosophila metamorphosis. Molecular cell. 2000; 5:445–455. [PubMed: 10882130]

Juhasz G, Hill JH, Yan Y, Sass M, Baehrecke EH, Backer JM, Neufeld TP. The class III PI(3)K Vps34 promotes autophagy and endocytosis but not TOR signaling in Drosophila. The Journal of cell biology. 2008; 181:655–666. [PubMed: 18474623]

Kato K, Awasaki T, Ito K. Neuronal programmed cell death induces glial cell division in the adult Drosophila brain. Development. 2009; 136:51–59. [PubMed: 19019992]

Kerr JF, Wyllie AH, Currie AR. Apoptosis: a basic biological phenomenon with wide-ranging implications in tissue kinetics. British journal of cancer. 1972; 26:239–257. [PubMed: 4561027]

Kimura KI, Truman JW. Postmetamorphic cell death in the nervous and muscular systems of Drosophila melanogaster. The Journal of neuroscience : the official journal of the Society for Neuroscience. 1990; 10:403-401. [PubMed: 2106014]

Koelle MR, Talbot WS, Segraves WA, Bender MT, Cherbas P, Hogness DS. The Drosophila EcR gene encodes an ecdysone receptor, a new member of the steroid receptor superfamily. Cell. 1991; 67:59–77. [PubMed: 1913820]

Lavorgna G, Karim FD, Thummel CS, Wu C. Potential role for a FTZ-F1 steroid receptor superfamily member in the control of Drosophila metamorphosis. Proceedings of the National Academy of Sciences of the United States of America. 1993; 90:3004–3008. [PubMed: 8096644]

Lee CY, Baehrecke EH. Steroid regulation of autophagic programmed cell death during development. Development. 2001; 128:1443–1455. [PubMed: 11262243]

Lee CY, Clough EA, Yellon P, Teslovich TM, Stephan DA, Baehrecke EH. Genome-wide analyses of steroid-and radiation-triggered programmed cell death in Drosophila. Current biology: CB. 2003; 13:350–357. [PubMed: 12593803]

Lee CY, Cooksey BA, Baehrecke EH. Steroid regulation of midgut cell death during Drosophila development. Developmental biology. 2002a; 250:101–111. [PubMed: 12297099]

Lee CY, Simon CR, Woodard CT, Baehrecke EH. Genetic mechanism for the stage- and tissue-specific regulation of steroid triggered programmed cell death in Drosophila. Developmental biology. 2002b; 252:138–148. [PubMed: 12453466]

Lockshin RA, Zakeri Z. Cell death in health and disease. Journal of cellular and molecular medicine. 2007; 11:1214–1224. [PubMed: 18031301]

Mizushima N, Noda T, Yoshimori T, Tanaka Y, Ishii T, George MD, Klionsky DJ, Ohsumi M, Ohsumi Y. A protein conjugation system essential for autophagy. Nature. 1998; 395:395–398. [PubMed: 9759731]

Ohno CK, Ueda H, Petkovich M. The Drosophila nuclear receptors FTZ-F1 alpha and FTZ-F1 beta compete as monomers for binding to a site in the fushi tarazu gene. Mol Cell Biol. 1994; 14:3166–3175. [PubMed: 8164672]

Ranganayakulu G, Schulz RA, Olson EN. Wingless signaling induces nautilus expression in the ventral mesoderm of the Drosophila embryo. Developmental biology. 1996; 176:143–148. [PubMed: 8654890]

Redt-Clouet C, Trannoy S, Boulanger A, Tokmatcheva E, Savvateeva-Popova E, Parmentier ML, Preat T, Dura JM. Mushroom body neuronal remodelling is necessary for short-term but not for long term courtship memory in Drosophila. Eur J Neurosci. 2012; 35:1684–1691. [PubMed: 22571719]

Riddiford LM, Cherbas P, Truman JW. Ecdysone receptors and their biological actions. Vitamins and hormones. 2000; 60:1–73. [PubMed: 11037621]

Robertson CW. The metamorphosis of Drosophila melanogaster, including an accurately timed account of the principal morphological changes. Journal of Morphology. 1936; 59:351–399.

Robinow S, Talbot WS, Hogness DS, Truman JW. Programmed cell death in the Drosophila CNS is ecdysone-regulated and coupled with a specific ecdysone receptor isoform. Development. 1993; 119:1251–1259. [PubMed: 8306887]

Roy S, VijayRaghavan K. Patterning muscles using organizers: larval muscle templates and adult myoblasts actively interact to pattern the dorsal longitudinal flight muscles of Drosophila. The Journal of cell biology. 1998; 141:1135–1145. [PubMed: 9606206]

Segraves WA, Hogness DS. The E75 ecdysone-inducible gene responsible for the 75B early puff in Drosophila encodes two new members of the steroid receptor superfamily. Genes & development. 1990; 4:204–219. [PubMed: 2110921]

Sullivan AA, Thummel CS. Temporal profiles of nuclear receptor gene expression reveal coordinate transcriptional responses during Drosophila development. Mol Endocrinol. 2003; 17:2125–2137. [PubMed: 12881508]

Talbot WS, Swyryd EA, Hogness DS. Drosophila tissues with different metamorphic responses to ecdysone express different ecdysone receptor isoforms. Cell. 1993; 73:1323–1337. [PubMed: 8324824]

Thomas HE, Stunnenberg HG, Stewart AF. Heterodimerization of the Drosophila ecdysone receptor with retinoid X receptor and ultraspiracle. Nature. 1993; 362:471–475. [PubMed: 8385270]

Thummel CS. From embryogenesis to metamorphosis: the regulation and function of Drosophila nuclear receptor superfamily members. Cell. 1995; 83:871–877. [PubMed: 8521511]

Thummel CS. Flies on steroids--Drosophila metamorphosis and the mechanisms of steroid hormone action. Trends in genetics: TIG. 1996; 12:306–310. [PubMed: 8783940]

Thummel CS. Molecular mechanisms of developmental timing in C. elegans and Drosophila. Developmental cell. 2001; 1:453–465. [PubMed: 11703937]

Truman JW, Talbot WS, Fahrbach SE, Hogness DS. Ecdysone receptor expression in the CNS correlates with stage-specific responses to ecdysteroids during Drosophila and Manduca development. Development. 1994; 120:219–234. [PubMed: 8119129]

Wasser M, Bte Osman Z, Chia W. EAST and Chromator control the destruction and remodeling of muscles during Drosophila metamorphosis. Developmental biology. 2007; 307:380–393. [PubMed: 17540360]

Winbush A, Weeks JC. Steroid-triggered, cell-autonomous death of a Drosophila motoneuron during metamorphosis. Neural Dev. 2011; 6:15. [PubMed: 21521537]

Woodard CT, Baehrecke EH, Thummel CS. A molecular mechanism for the stage specificity of the Drosophila prepupal genetic response to ecdysone. Cell. 1994; 79:607–615. [PubMed: 7954827]

Yang Z, Klionsky DJ. An overview of the molecular mechanism of autophagy. Current topics in microbiology and immunology. 2009; 335:1–32. [PubMed: 19802558]

Yang Z, Klionsky DJ. Mammalian autophagy: core molecular machinery and signaling regulation. Curr Opin Cell Biol. 2011; 22:124–131. [PubMed: 20034776]

Yao TP, Segraves WA, Oro AE, McKeown M, Evans RM. Drosophila ultraspiracle modulates ecdysone receptor function via heterodimer formation. Cell. 1992; 71:63–72. [PubMed: 1327536]

Yorimitsu T, Klionsky DJ. Autophagy: molecular machinery for self-eating. Cell Death Differ. 2005; 12(Suppl 2):1542–1552. [PubMed: 16247502]

Zirin J, Perrimon N. Drosophila as a model system to study autophagy. Semin Immunopathol. 2010; 32:363–372. [PubMed: 20798940]

Highlights

- Ecdysone receptor isoform B1 is required cell autonomously for abdominal muscle death
- Orphan nuclear receptor FTZ-F1 expression determines the timing of muscle death
- Abdominal muscle death occurs by apoptosis, and does not require autophagy

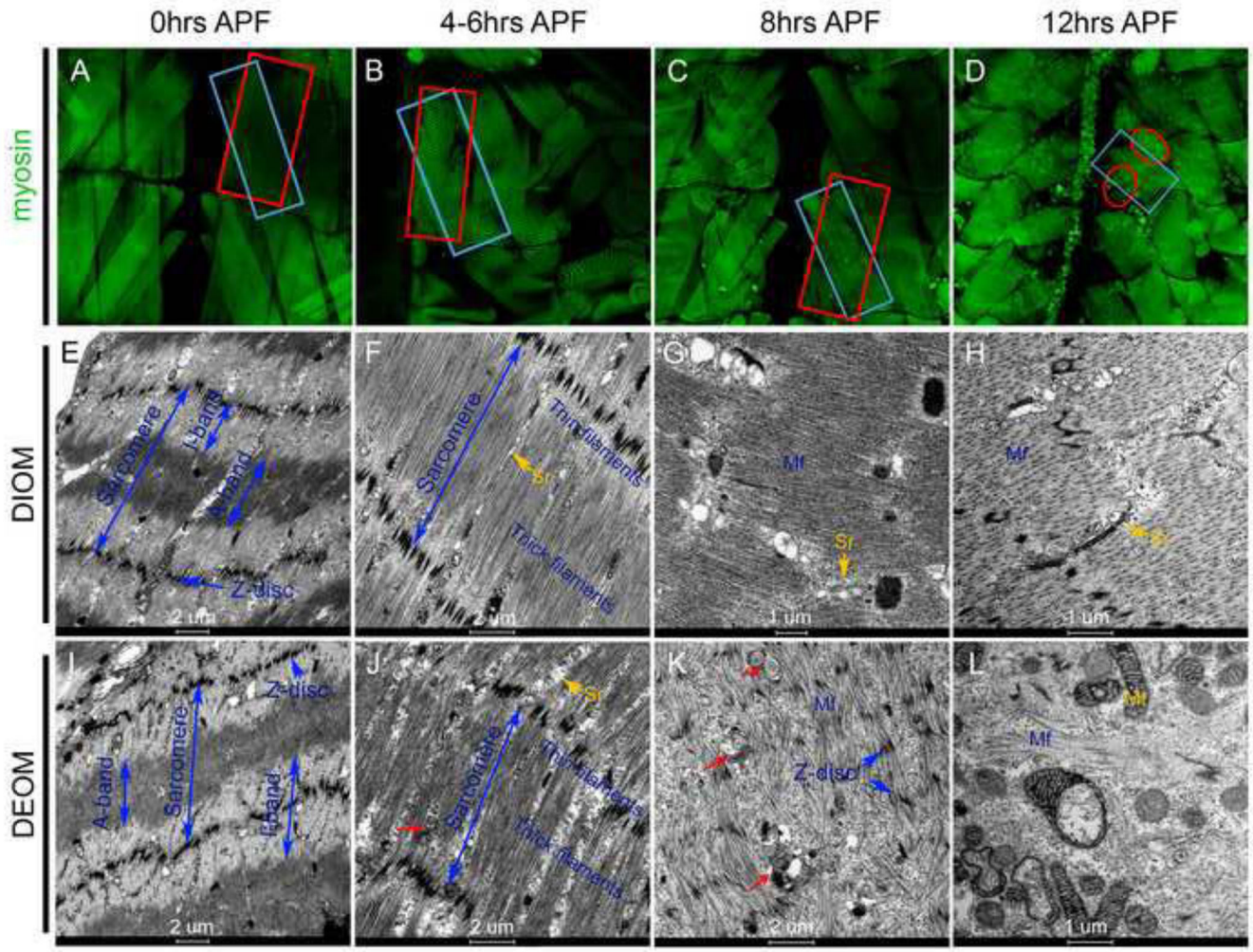

Figure 1. Time course of degenerating and persistent muscles during metamorphosis

(A–D) Abdominal muscles from the *weeP26* transgenic line, expressing a GFP-tagged Myosin heavy chain protein (green). The dorsal external oblique muscle (DEOM) is marked with a red outline. The dorsal internal oblique muscle (DIOM) is marked with blue outline. (A) At 0hrs and (B) 4–6hrs after puparium formation (APF), both DIOMs and DEOMs maintain their larval muscle morphology. (C) At 8hrs APF the DEOMs, but not the DIOMS, begin to show signs of muscle degradation, as the muscles round up and the myosin pattern is disrupted. (D) By 12hrs APF the DIOMs are more compact, but retain an orderly myosin pattern, while the DEOMs are almost completely disintegrated. (E–H) Electron micrographs (EM) of DIOMs from 0–12hrs APF showing maintenance of the sarcomere throughout this period. (I–L) EM of DEOMs from 0–12hrs APF. (I) At 0hrs and (J) 4–6hrs APF the muscles retain their larval sarcomere pattern, and vesicles occasionally appear between the myofibrils (red arrow). (K) At 8hrs APF, myofibrils are present, but are disorganized, while vesicles and multi-vesicular bodies (red arrows) are more prevalent. (L) By 12hrs APF, almost all myofibrils are gone. Abbreviations: Mf (myofibrils), Sr (sarcoplasmic reticulum), Mt (mitochondria).

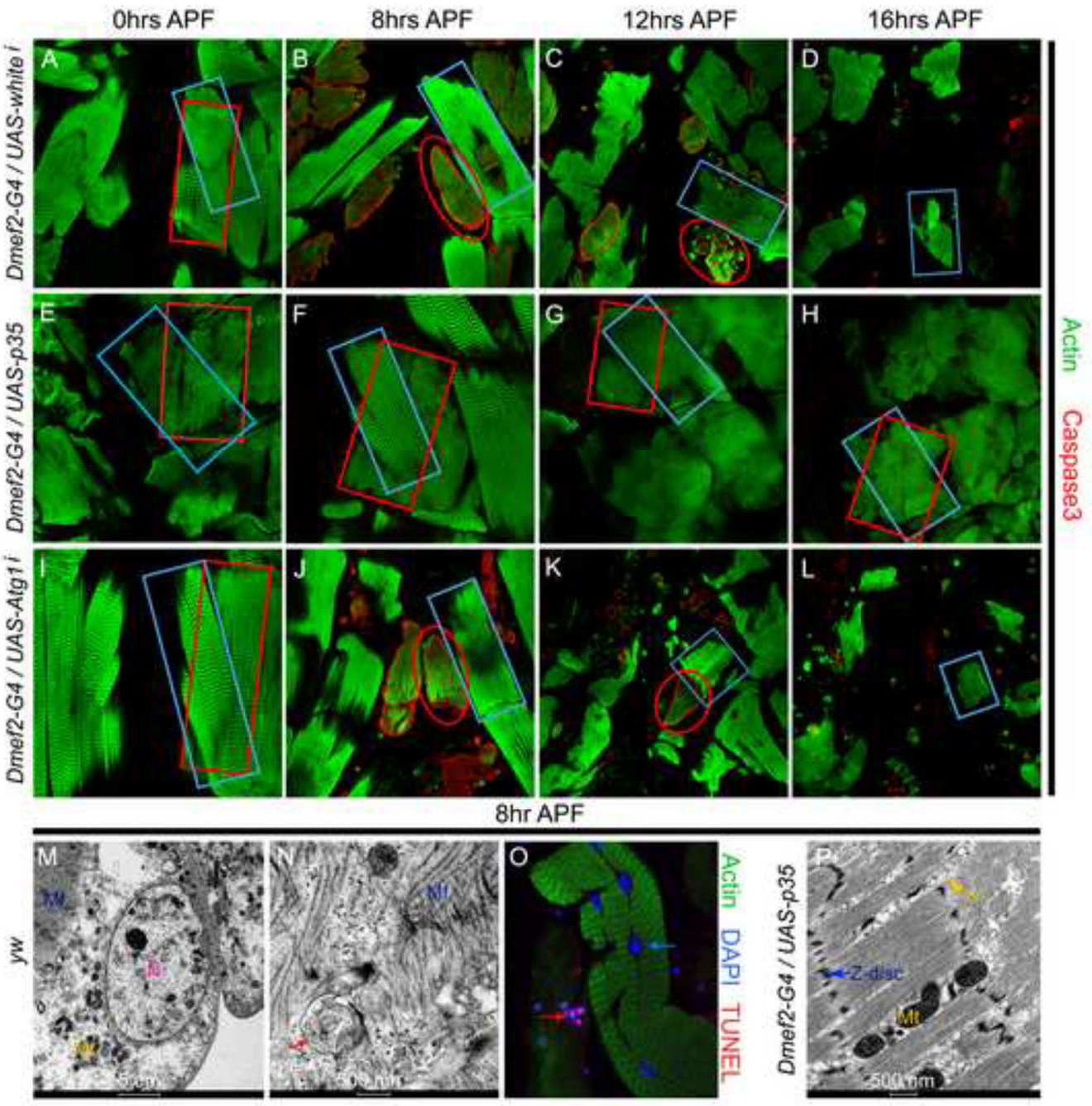

Figure 2. DEOM histolysis requires caspase activity but not autophagy

(A–L) Time course of abdominal muscles stained with Phalloidin/actin (green) and a-cleaved caspase3 (red). In all panels the red outline indicates the DEOM and the blue outline the DIOM. (A–D) Muscles from control *Dmef2-Gal4/UAS-white RNAi (UAS-white i)* larvae. DIOMs show no caspase activity at any time point, while the degrading DEOMs show caspase staining beginning at 8hrs APF (B) through their disintegration at 12hrs APF (C). (E–H) Muscles from *Dmef2-Gal4/UAS-p35* larvae. DEOMs show no cleaved caspase staining and fail to degrade, although like the DIOMs, they become smaller by 16hrs APF

(H). (I–L) Muscles from *Dmef2-Gal4/UAS-Atg1 RNAi* larvae. Inhibition of autophagy has no effect on the timing of caspase activity in the DEOMs nor on their degradation. (M) EM of DEOM nucleus from a *yw* (control) larva at 8hrs APF. Note the condensed chromatin characteristic of apoptosis. (N) EM of DEOM cytoplasm from a *yw* larva at 8hrs APF. The red arrow points to a vesicle containing cytoplasmic debris. (O) TUNEL staining of DIOM and DEOM from a *yw* larva at 8hrs APF. TUNEL stain marks the shrunken nuclei of the degrading DEOM (red arrow), but not the nuclei of the persistent DIOM (blue arrow). Blue=DAPI, red=TUNEL, green=actin. (P) EM of DEOM from *Dmef2-Gal4/UAS-p35* larvae at 8hrs APF. Expression of p35 inhibits the degradation of the sarcomere (compare to panel N). APF Abbreviations: Mf (myofibrils), Sr (sarcoplasmic reticulum), Mt (mitochondria), N (Nucleus).

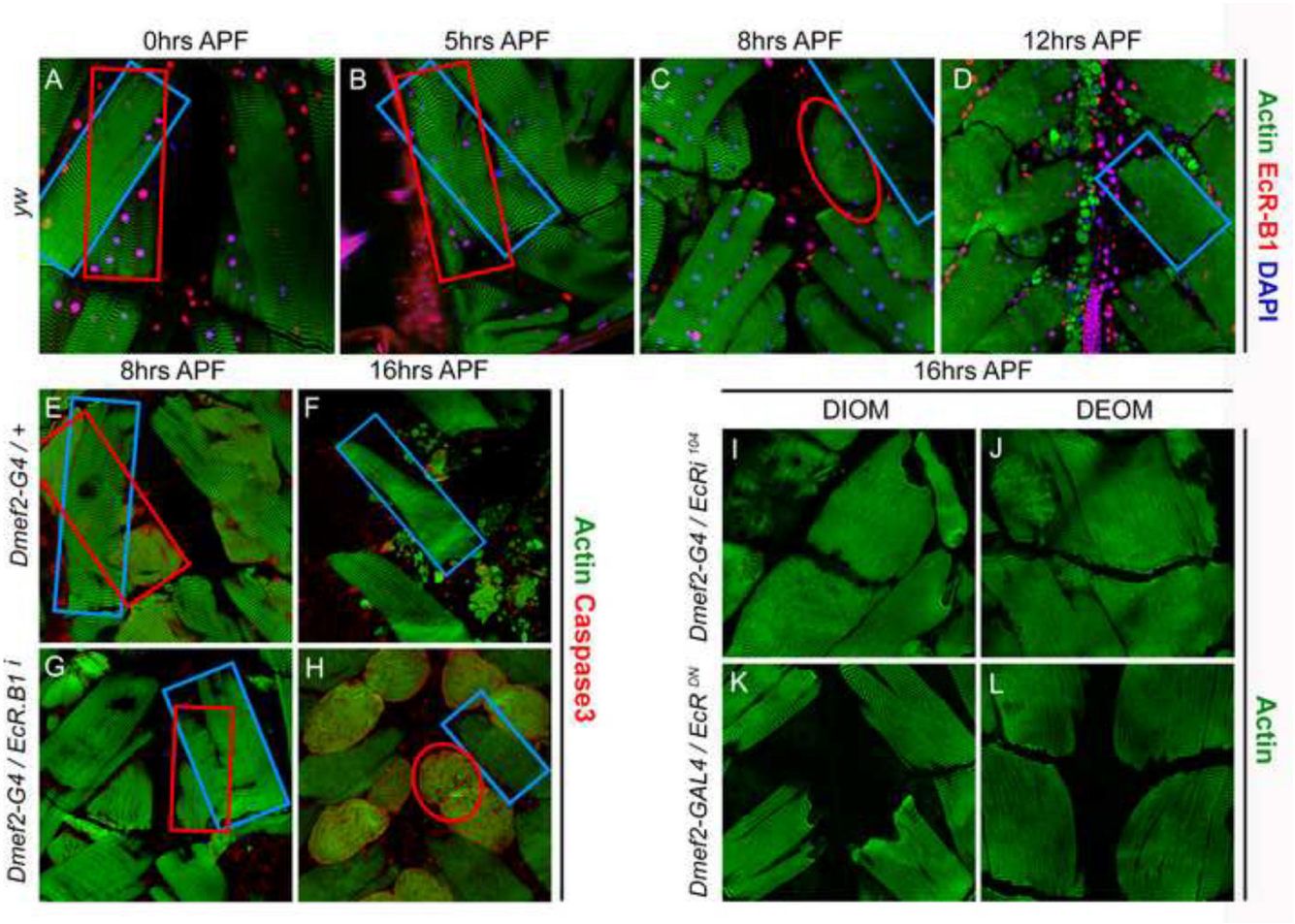

Figure 3. Ecdysone signaling is required for DEOM histolysis

(A–D) Time course of abdominal muscles from a *yw* larvae stained with α-EcR-B1 (red), Phalloidin/actin (green), and DAPI (blue). In all panels the red outline indicates the DEOM and the blue outline indicates the DIOM. Both DEOMs and DIOMs express EcR-B1 throughout the period of muscle histolysis. (E–H) Abdominal muscles at 8hrs APF and 16hrs APF stained with Phalloidin/actin (green) and a-cleaved caspase3 (red). DEOMs from *Dmef2-Gal4/UAS-EcR-B1 RNAi* (G–H) show no cleaved caspase staining at 8hrs APF and degradation is reduced at 16hrs APF compared to *Dmef2-Gal4* muscles (E–F). (I–J) Abdominal muscles at 16hrs from *Dmef2-Gal4/UAS-EcR RNAi*^{104} larvae, stained with Phalloidin/actin (green). Both DIOM (I) and DEOM (J) persist with no signs of degradation. (K–L) Abdominal muscles at 16hrs from *Dmef2-Gal4/UAS-EcR*^{DN} larvae, stained with Phalloidin/actin (green). Similar to EcR knockdown, *EcR*^{DN} expression causes both DIOM (K) and DEOM (L) to persist with no signs of degradation.

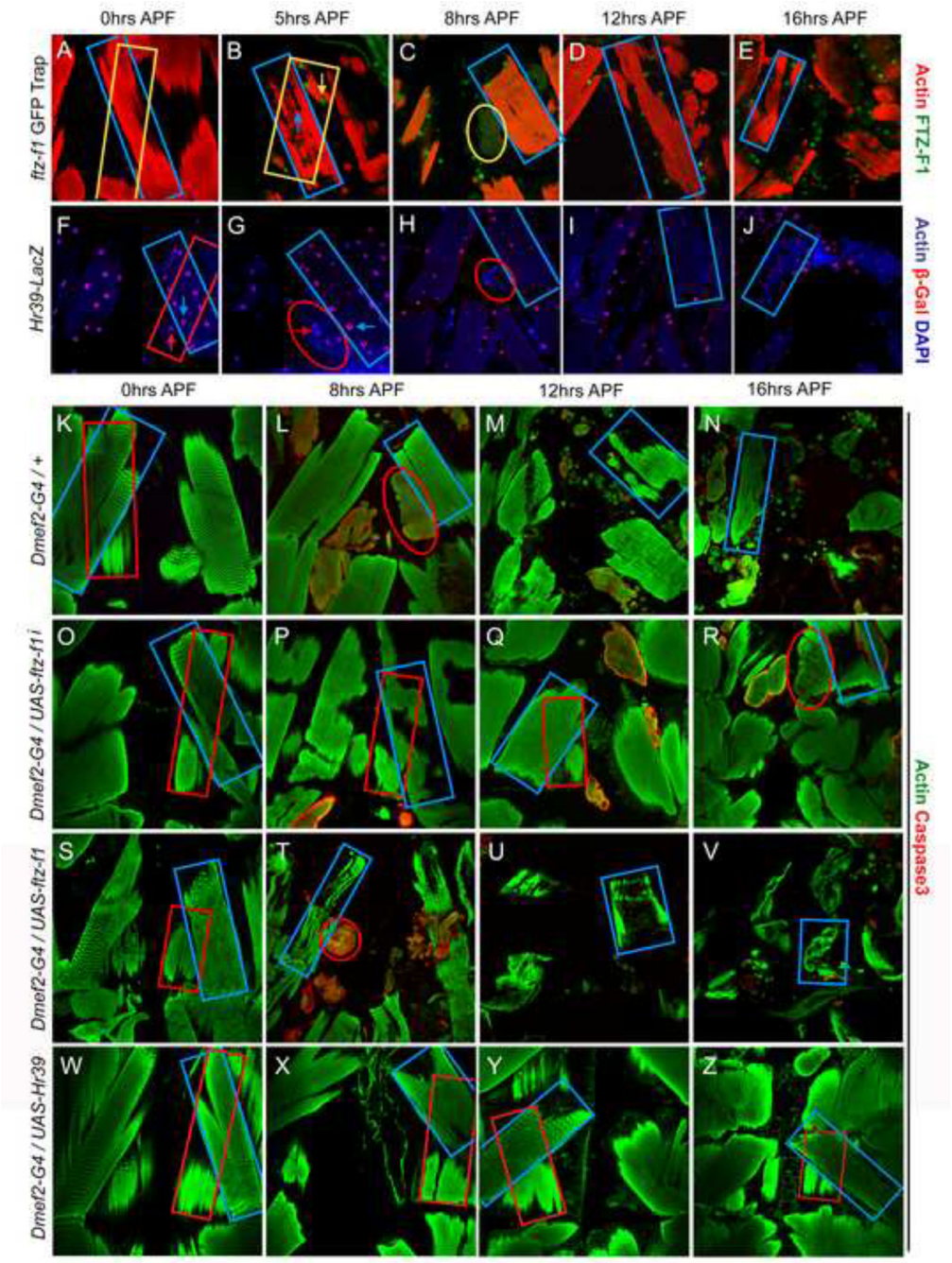

Figure 4. FTZ-F1 and HR39 have opposing effects on DEOM histolysis

(A–E) Time course of abdominal muscles from Flytrap line *YB0007*, in which GFP-tagged FTZ-F1 is expressed under the control of its endogenous promoter and enhancer elements. Larvae are stained with Phalloidin/actin (red). In all panels the blue outline indicates the DIOM and the yellow or red outline indicates the DEOM. At 5hrs APF (B) FTZ-F1-GFP localizes to the nuclei of the DEOMs (yellow arrow) but is absent from the DIOMs (blue arrow). At 8hrs APF (C) FTZ-F1-GFP localizes to both DIOMs and DEOMs, and persists in the DIOMs. (F–J) Time course of abdominal muscles expressing an *Hr39-lacZ* reporter,

stained with Phalloidin/actin and DAPI (blue) and α-β-gal (red). At 0hrs APF (F) and 8hrs APF (G), *Hr39-lacZ* is expressed strongly in the DIOMs (blue arrows), but weakly in the DEOMs (red arrows). (H–J) *HR39-lacZ* expression persists in the DIOMs through 16hrs APF. (K–Z) Time course of abdominal muscles stained with a-cleaved caspase3 (red) and Phalloidin/actin (green). (K–N) In control *Dmef2-Gal4* animals, caspase staining appears at 8hrs APF (L) in the degrading DEOMs. (O–R) In *Dmef2-Gal4/UAS-ftz-f1 RNAi* animals, caspase activation is repressed in DEOMs, which often persist through 16hrs APF. (S–V) In *Dmef2-Gal4/UAS-ftz-f1* over-expression animals, DEOMs are prematurely degraded at 8hrs APF (T), while the DIOMs are thinner, but still fail to activate caspase through 16hrs APF. (W–Z) In *Dmef2-Gal4/UAS-Hr39* over-expression animals, neither DEOMs nor DIOMs activate caspase or are degraded through 16hrs APF.

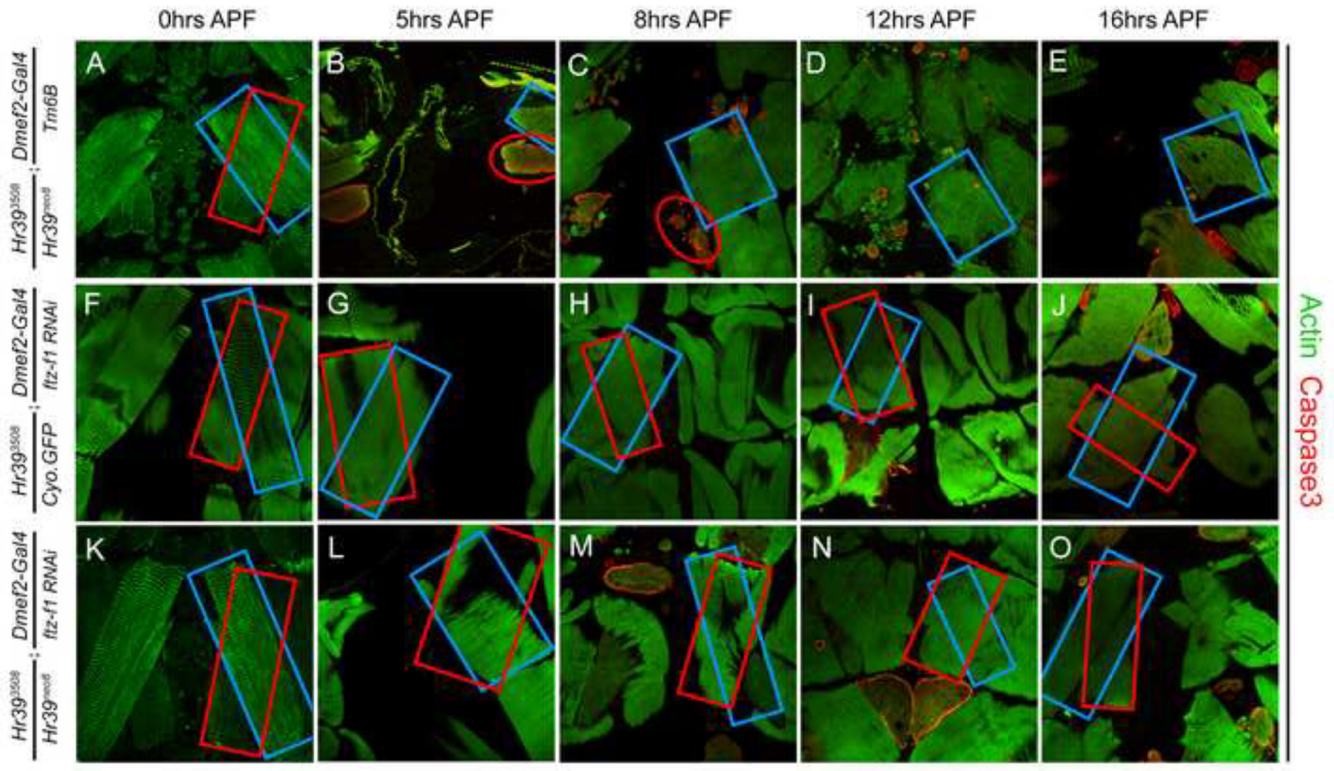

Figure 5. *ftz-f1* is epistatic to *Hr39*

(A–O) Time course of abdominal muscles stained with a-cleaved caspase3 (red) and Phalloidin/actin (green). In all panels the blue outline indicates the DIOM and the red outline the DEOM. (A–E) DEOMs from *Hr39*^{3508}*/Hr39*^{neo8}*; Dmef2-Gal4/TM6B* larvae degenerate prematurely. At 5hrs APF (B) the DIOMs have activated caspase, and by 8hrs APF (C) the muscles are almost completely degraded. (F–J) DEOMs from *Hr39*^{3508}*/ CyO.GFP; Dmef2-Gal4/UAS-ftz-F1 RNAi* larvae show delayed caspase activation and degradation, similar to *Dmef2-Gal4/UAS-ftz-F1 RNAi* larvae (see Figure 4O–R). (K–O) DEOMs from *HR39*^{3508}*/HR39*^{neo8}*; Dmef2-Gal4/UAS-ftz-F1 RNAi* larvae show also show a delayed degradation phenotype, more like the *ftz-f1 RNAi* than the *Hr39* mutant.